

AD-A192 739

A SIMULATION ANALYSIS OF ERRORS IN THE MEASUREMENT OF
STANDARD ELECTROCHE. (U) PURDUE UNIV LAFAYETTE IN DEPT
OF CHEMISTRY D F MILNER ET AL. 30 SEP 87 TR-63

1/1

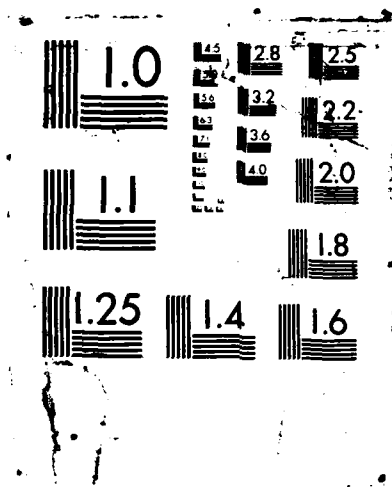
UNCLASSIFIED

N00014-86-K-0556

F/G 7/4

NL





AD-A192 739

DTIC FILE COPY ①

OFFICE OF NAVAL RESEARCH

Contract N00014-86-K-0556

Technical Report No. 63

A Simulation Analysis of Errors in the Measurement of
Standard Electrochemical Rate Constants from
Phase-Selective Impedance Data

by

D. F. Milner and M. J. Weaver

Prepared for Publication

in the

Journal of Electroanalytical Chemistry

222, 21-33 (1987)

Purdue University

Department of Chemistry

West Lafayette, Indiana 47907

September 25, 1987

DTIC
ELECTE
MAR 24 1988
S E D

Reproduction in whole, or in part, is permitted for any purpose of the United States Government.

* This document has been approved for public release and sale: its distribution is unlimited.

88 3 22 092

REPORT DOCUMENTATION PAGE

1a REPORT SECURITY CLASSIFICATION Unclassified			1b RESTRICTIVE MARKINGS		
2a SECURITY CLASSIFICATION AUTHORITY			3 DISTRIBUTION/AVAILABILITY OF REPORT Approved for public release and sale; its distribution is unlimited.		
2b DECLASSIFICATION/DOWNGRADING SCHEDULE					
4 PERFORMING ORGANIZATION REPORT NUMBER(S) Technical Report No. 63			5 MONITORING ORGANIZATION REPORT NUMBER(S)		
6a NAME OF PERFORMING ORGANIZATION Purdue University Department of Chemistry		6b OFFICE SYMBOL (If applicable)		7a NAME OF MONITORING ORGANIZATION Division of Sponsored Programs Purdue Research Foundation	
6c ADDRESS (City, State, and ZIP Code) Purdue University Department of Chemistry West Lafayette, IN 47907				7b ADDRESS (City, State, and ZIP Code) Purdue University West Lafayette, Indiana 47907	
8a NAME OF FUNDING/SPONSORING ORGANIZATION Office of Naval Research		8b OFFICE SYMBOL (If applicable)		9 PROCUREMENT INSTRUMENT IDENTIFICATION NUMBER Contract No. N00014-86-K-0556	
8c ADDRESS (City, State, and ZIP Code) 800 N. Quincy St. Arlington, VA 22217		10 SOURCE OF FUNDING NUMBERS			
		PROGRAM ELEMENT NO		PROJECT NO	TASK NO
					WORK UNIT ACCESSION NO
11 TITLE (Include Security Classification) A Simulation Analysis of Errors in the Measurement of Standard Electrochemical Rate Constants from Phase-Selective Impedance Data					
12 PERSONAL AUTHOR(S) D. F. Milner and M. J. Weaver					
13a TYPE OF REPORT Technical		13b TIME COVERED FROM 10/1/86 TO 9/30/87		14 DATE OF REPORT (Year, Month, Day) September 25, 1987	
15 PAGE COUNT					
16 SUPPLEMENTARY NOTATION					
17 COSATI CODES			18 SUBJECT TERMS (Continue on reverse if necessary and identify by block number)		
FIELD	GROUP	SUB-GROUP	digital simulation analysis, AC impedance, electrochemical rate constants		
19 ABSTRACT (Continue on reverse if necessary and identify by block number) A digital simulation analysis is presented of the coupled effects of solution resistance and lock-in amplifier damping upon the evaluation of standard rate constants, k_{ob}^s , for rapid electrode reactions using phase-selective AC impedance measurements with positive-feedback IR compensation. These two effects combine so to yield "apparent" (i.e. measured) rate constants, k_{ob}^s (app), evaluated using the conventional frequency-dependent analysis that are generally smaller than the actual values, k_{ob}^s (true). The extent to which these systematic errors depend on experimental conditions is explored for various values of k_{ob}^s (true), the uncompensated and specific solution resistances, the amplifier filter time constant, the double-layer capacitance and other relevant parameters. A simple scheme employing these simulations is outlined by which k_{ob}^s (true) values can be extracted from k_{ob}^s (app) measurements. Some experimental verification of these effects is also presented.					
20 DISTRIBUTION/AVAILABILITY OF ABSTRACT <input checked="" type="checkbox"/> UNCLASSIFIED/UNLIMITED <input checked="" type="checkbox"/> SAME AS RPT <input type="checkbox"/> DTIC USERS			21 ABSTRACT SECURITY CLASSIFICATION		
22a NAME OF RESPONSIBLE INDIVIDUAL			22b TELEPHONE (Include Area Code)		22c OFFICE SYMBOL

A Simulation Analysis of Errors in the
Measurement of Standard Electrochemical Rate Constants from
Phase-Selective Impedance Data

David F. Milner and Michael J. Weaver

Department of Chemistry

Purdue University

West Lafayette, Indiana 47907 (U.S.A.)

ABSTRACT

A digital simulation analysis is presented of the coupled effects of solution resistance and lock-in amplifier damping upon the evaluation of standard rate constants, k_{ob}^s , for rapid electrode reactions using phase-selective AC impedance measurements with positive-feedback iR compensation. These two effects combine so to yield "apparent" (i.e. measured) rate constants, $k_{ob}^s(\text{app})$, evaluated using the conventional frequency-dependent analysis that are generally smaller than the actual values, $k_{ob}^s(\text{true})$. The extent to which these systematic errors depend on experimental conditions is explored for various values of $k_{ob}^s(\text{true})$, the uncompensated and specific solution resistances, the amplifier filter time constant, the double-layer capacitance, and other relevant parameters. A simple scheme employing these simulations is outlined by which $k_{ob}^s(\text{true})$ values can be extracted from $k_{ob}^s(\text{app})$ measurements. Some experimental verification of these effects is also presented.

Accession For	
NTIS GRA&I	<input checked="" type="checkbox"/>
DTIC TAB	<input type="checkbox"/>
Unannounced	<input type="checkbox"/>
Justification	
By _____	
Distribution/	
Availability Codes	
Avail and/or	Special
101	

A-1



The measurement of rate constants for electron exchange of redox couples at metal-solution interfaces (so-called "standard" electrochemical rate constants, k_{ob}^s) has long been a matter of fundamental interest.¹ A large and important class of reactions involve redox couples for which the inner-shell barrier (i.e., that arising from structural differences between the redox forms) is negligible or small, so that the activation energy ΔG^* arises predominantly from outer-shell (solvent) reorganization. Current interest in such processes, as well as in self-exchange reactions in homogeneous solution, centers on the anticipated important contribution of solvent dynamics to the preexponential factor.² For such systems the k_{ob}^s is predicted to approach and possibly surpass the maximum values amenable to experimental evaluation, even when using rapid perturbation techniques. Consequently, under these circumstances, estimates of k_{ob}^s obtained using such methods may be entirely erroneous. It is therefore of paramount importance to both identify and quantify the various experimental factors that determine this upper limit when using a given instrument and electrochemical technique.

A primary method used to evaluate such rapid electrochemical rate constants involves AC impedance measurements with phase-selective detection.^{3,4} The contributions of Don Smith in this area are well known;³ his work has had a central influence on the development of such AC methods and their broadbased application in electrochemistry, including applications to electrode kinetics. The cell impedance as a function of the AC frequency and the electrode potential can provide a particularly straightforward route to the determination of k_{ob}^s . The technique as it is commonly practiced utilizes a potentiostat with positive-feedback IR

lock-in amplifier employed as a phase-sensitive detector, and either a dropping mercury electrode (DME) or a stationary mercury or solid surface for the working electrode.

Of the various factors that can conspire to produce a significant and ultimately limiting impediment to the reliable determination of k_{ob}^s , the influence of solution resistance, R_s , is paramount. Besides the common use of positive-feedback iR compensation, the presence of R_s is accounted for in a.c. impedance measurements by means of a vectorial subtraction scheme, originally due to Randles.⁵ However, in both these approaches the very presence of R_s will place inevitable limitations on the values of k_{ob}^s that can be reliably evaluated, especially for large R_s values. Analyses dealing with the manner and extent to which these limitations occur in practice have, nevertheless, remained surprisingly sparse.

We present here in some detail a digital simulation analysis of this problem, primarily as applied to a.c. impedance measurements employing positive-feedback iR compensation. We have briefly reported previously a simple approach which can enable estimates of the error induced in k_{ob}^s measurements using the conventional analysis, based on simulations using trial values of R_s and the double-layer capacitance, C_{dl} .⁶ The present report contains a development of this analysis, and also provides estimates of the additional measurement error that can be induced by the solution resistance when coupled with damping in the lock-in amplifier. Some experimental verification of these effects is also presented. The origin and magnitude of the errors from measuring the AC currents themselves that result from amplifier damping are detailed in a separate paper.⁷

The overall aim of this work is to aid the experimentalist in

ascertaining the validity as well as the quantitative accuracy of fast electrode kinetic measurements made using phase-selective a.c. detection. Taken together, we believe that these analyses provide a relatively straightforward means by which the influence of these undesired solution resistance and amplifier damping effects can be diagnosed as well as minimized.

Simulation Procedures

The general approach employed here involves producing digital simulations of the AC current, including the time dependence at a growing DME, at a given fixed potential either in the presence or the absence of an electroactive species.

We employ the conventional equivalent circuit model of an electrochemical cell as it is formulated for simple redox processes in the AC experiment, shown schematically in Fig. 1. (This model, originally due to Randles,⁵ is generally accepted as a reasonable approximation.⁸) It is readily apparent that the cell impedance is given by:

$$Z_{\text{cell}} = \left(\frac{1}{Z_{\text{Cdl}}} + \frac{1}{R_F + Z_{\text{CF}}} \right) + R_{\text{us}} \quad (1)$$

where R_{us} is the uncompensated solution resistance (i.e. that part of the total system resistance which has not been compensated for electronically), R_F is the resistive part of the faradaic impedance, Z_{Cdl} is the impedance of the double-layer capacitance, and Z_{CF} is the impedance of the capacitive part of the faradaic impedance.

The impedance of a capacitance C_1 is given by:

$$Z_{C_1} = -j (\omega C_1)^{-1} \quad (2)$$

where ω is the radial frequency, and j is the unit irrational constant ($\sqrt{-1}$).

For the DME, one must consider the time dependence of the electrode area, A . Besides the obvious proportionality between C_{dl} and A , the solution resistance, and thus the uncompensated resistance, of an electrochemical cell is also a function of A provided that the level of compensation is not altered as the area varies. For a spherical electrode, such as is approximated by a DME, the uncompensated resistance as a function of surface area is given by:⁹

$$R_{us} = R_{hom} + \rho(4\pi A)^{-1/2} \quad (3)$$

where ρ is the specific solution resistance, R_{hom} is the "homogeneous" part of the resistance (that portion which is independent of the electrode area) and R_{us} is the uncompensated solution resistance. Since the term $\rho(4\pi A)^{-1/2}$ represents the resistance between a spherical electrode and a reference electrode in the bulk solution, R_{hom} is approximately zero in the absence of iR compensation.⁹

Equations describing R_F and C_F resulting from the presence of the electroactive species are also necessary. These can be expressed as:^{3a}

$$R_F = (\omega C_F)^{-1} [1 + (2\omega^{1/2}/\lambda)] \quad (4)$$

where

$$\lambda = (k_{ob}^s/D^{1/2}) \left(\exp\left[-\frac{\alpha nF}{RT} (E-E^\circ)\right] + \exp\left\{(1-\alpha) \frac{nF}{RT} (E-E^\circ)\right\} \right) \quad (4a)$$

$$C_F = \frac{\omega n^2 F^2 A C^* (2\omega D)^{1/2}}{4RT \cosh^2(RT/2nF)(E-E^\circ)} \quad (5)$$

In these equations, D is the reactant diffusion coefficient, α is the cathodic transfer coefficient, n is the number of electrons, E is the electrode potential, E° is the standard potential of the redox couple, and

A is the electrode area.

In the DME case, the time dependence of A is given by:

$$A = 4\pi(3mt/4\pi\sigma)^{2/3} \quad (6)$$

where m and σ are the mercury flow rate and density, and t is the time since drop birth.

These relations enable us to digitally simulate in-phase and quadrature currents as a function of $(E-E^*)$ and the applied frequency ω , for various input parameters, notably k_{ob}^s , R_s (R_{us} when iR compensation is involved), and C_{dl} . For simplicity, parameters which have a minor or easily predictable impact upon the results were held constant at the following typical values: $D = 10^{-5} \text{ cm}^2 \text{ s}^{-1}$, $C^* = 1 \text{ M}$, $m = 3 \text{ mg s}^{-1}$, t_D (the mercury drop time) = 2s, $T = 300\text{K}$, $n = 1$, $\alpha = 0.5$, and E_{AC} (the rms amplitude of the applied AC signal) = 2.24mV.

These simulated impedance data were then used to obtain "apparent" values of k_{ob}^s , $k_{ob}^s(\text{app})$, using the conventional analysis involving the frequency-dependence of the phase angle.^{3a} Specifically, the cotangent of the phase angle, $\cot \phi$, was taken to be:

$$\cot \phi = I_Q^{\text{cor}} / I_I^{\text{cor}} \quad (7)$$

where I_Q^{cor} and I_I^{cor} are the simulated quadrature and in-phase currents corrected for the corrected background currents sufficiently far from the AC polarographic wave so that faradaic currents are negligible. The $\cot \phi$ values were then plotted against $\omega^{1/2}$, and the slope of the resulting regression line, s, used to obtain $k_{ob}^s(\text{app})$ from^{3a}:

$$k_{ob}^s(\text{app}) = (2D)^{1/2} / sG \quad (8)$$

where

$$G = (\exp \alpha)/(1 + \exp \alpha) \quad (8a)$$

The quantity $k_{ob}^s(\text{app})$ is therefore the rate constant that would be extracted from AC impedance measurements with an electrochemical cell having equivalent circuit components equal to the simulation input parameters. The extent to which $k_{ob}^s(\text{app})$ differs from the "true" value, $k_{ob}^s(\text{true})$, represents the systematic error which will necessarily occur when the conventional analysis is employed under a given set of experimental conditions.⁷ In terms of the present analysis, two factors will cause $k_{ob}^s(\text{app})$ to differ from $k_{ob}^s(\text{true})$. Firstly, when the uncompensated solution resistance, R_{us} , is not exactly zero, the conventional analysis embodied in Eq. (7)-(8) is not strictly valid. The extent of the resulting error clearly depends upon R_{us} ; the simulation results given below provide a means of estimating the magnitude of the correction to $k_{ob}^s(\text{app})$ that is required.

An additional source of error in determining k_{ob}^s if significant time-dependent currents are involved (most commonly when using a DME) arises from the distortion in the measurement of time-dependent in-phase and quadrature currents using a lock-in amplifier that results from a damping effect. The distortion of the signal caused by the bandwidth-limiting portion of the lock-in amplifier, namely the low-pass filter stages following the balanced mixer, can be described by^{7,10}

$$V(t) = (RC)^{-1} \int_{-\infty}^t V_i(\tau) \exp[-(t-\tau)/RT] d\tau \quad (9)$$

where $V(t)$ and $V_i(t)$ are the voltage at the filter output and input,

respectively, at time t , and RC is the filter time constant. It is apparent from Eq. (9) that for the simple RC low-pass filters used in most commercial lock-in amplifiers, the resulting absolute error in the measured current is approximately proportional to the time derivative of the detected signal. Further details of this aspect of the simulations are given elsewhere.⁷ Such damping effects turn out to be of significance even when $R_{us} = 0$ if relatively high-resistance media (i.e. high ρ) are employed.

RESULTS AND DISCUSSION

The uncompensated solution resistance, R_{us} , may be regarded as being a resistive component in series with the electrochemical double layer. If the AC cell current is non-zero, this resistance will in general prevent the phase of the double-layer potential from equalling that of the AC potential applied to the cell. If R_{us} is positive, the phase angle of the double-layer potential will be between 0° and -90° with respect to the applied potential in AC voltammetric measurements. Since the phase angle of the double-layer potential is negative, the measured phase angle of the faradaic current will then be less than that with respect to the actual double-layer potential. This results in larger values for $\cot \phi$, a greater regression slope, and thus smaller values of $k_{ob}^s(\text{app})$ than $k_{ob}^s(\text{true})$. We will now examine quantitatively the effects of positive R_{us} values, as these are predicted to,¹¹ and in our laboratory do, arise more frequently than negative values for R_{us} .

Effects of Uncompensated Resistance at a Stationary Electrode

The case of a stationary electrode will be considered first since the

effects of lock-in amplifier damping will usually then be absent. In addition to the fixed simulation parameters noted above, we set $A = 0.028 \text{ cm}^2$, which is the area obtained for a DME at the end of drop life using the previously quoted values for m and t_p . Simulations are presented here for two (typically "small" and "moderate") values of the double-layer capacitance, C_{dl} , 5 and $20 \mu\text{F cm}^{-2}$. In the absence of amplifier damping effects, the magnitude of the total solution resistance will not directly affect the simulation results, since only the uncompensated component R_{us} will cause $k_{ob}^s(\text{app})$ to differ from $k_{ob}^s(\text{true})$.

It is useful to consider simulations aimed at estimating the upper limit to k_{ob}^s that can be obtained for a particular electrode - electrolyte arrangement, as dictated by the minimum R_{us} value that can be achieved. This is most simply gleaned from the values of $k_{ob}^s(\text{app})$, which we label $k_{ob}^s(\text{app,lim})$, that are extracted from simulated data with $k_{ob}^s(\text{true})$ taken as infinity (i.e., immeasurably large). The experimental observation of $k_{ob}^s(\text{app})$ values that approach $k_{ob}^s(\text{app,lim})$ for a particular experimental arrangement provide a clear diagnosis of significant errors in $k_{ob}^s(\text{app})$ arising from a non-negligible R_{us} value.

Curve A of Fig. 2 is a plot of $k_{ob}^s(\text{app,lim})$ versus $\log R_{us}$ in the absence of amplifier damping effects, and for $C_{dl} = 5 \mu\text{F cm}^{-2}$. This plot clearly shows that even a small value of uncompensated solution resistance can be a serious impediment to the measurement of k_{ob}^s for a rapid reaction. For example, the $k_{ob}^s(\text{app,lim})$ value with only 1Ω of uncompensated solution resistance is 15 cm s^{-1} . For a more typical value of 3 ohms for R_{us} , such as is commonly attainable using a PAR 173/179 potentiostat, for example, the value of $k_{ob}^s(\text{app,lim})$ decreases to 5 cm s^{-1} . Even larger values of

R_{us} are to be expected experimentally as one moves to less polar, and hence more resistive solvents, with the increased possibility that the intended measurement of k_{ob}^s will contain information only on the magnitude of R_{us} rather than on the reaction rate.

Curve A of Fig. 3 illustrates the corresponding relationship between $k_{ob}^s(\text{app,lim})$ and $\log R_{us}$ for $C_{dl} = 20 \mu\text{F cm}^{-2}$. While this curve appears to have the same qualitative shape as curve A of Fig. 2, the decrease in $k_{ob}^s(\text{app,lim})$ with increasing R_{us} is significantly steeper in Fig. 3. Over the R_{us} range examined, 0.5 to 100 Ω , the values of $k_{ob}^s(\text{app,lim})$ for $C_{dl} = 5 \mu\text{F cm}^{-2}$ are about twice the corresponding value for $C_{dl} = 20 \mu\text{F cm}^{-2}$. This increase in the degree of distortion for larger C_{dl} is due solely to the increased nonfaradaic AC current which must flow through the uncompensated solution resistance, causing a greater phase shift in the double-layer potential.

In order to provide a more quantitative estimate of these errors, it is useful to examine the relation between $k_{ob}^s(\text{app})$ and $k_{ob}^s(\text{true})$ for particular R_{us} values. Curve A of Fig. 4 is a plot of $\log k_{ob}^s(\text{app})$ versus $k_{ob}^s(\text{true})$ for $R_{us} = 2 \Omega$, again in the absence of amplifier damping. As might be expected, it is seen that the relative error in $k_{ob}^s(\text{app})$ is relatively small for $k_{ob}^s(\text{true}) \leq 0.5 \text{ cm s}^{-1}$, and increases rapidly for larger rate constants as k_{ob}^s reaches the asymptotically limiting value, $k_{ob}^s(\text{app,lim})$.

Having exposed the degree to which relatively small R_{us} values can cause substantial errors in k_{ob}^s measurements using the conventional analysis based on the dependence of $\cot\phi$ upon $\omega^{1/2}$, it is reasonable to inquire if such errors can be diagnosed from the $\cot\phi$ - $\omega^{1/2}$ plots themselves.

That this is indeed the case is illustrated in Fig. 5, which shows simulated $\cot\phi-\omega^{1/2}$ plots obtained for several values of R_{us} (0, 0.5, 1, and 2 Ω), again with $k_{ob}^s(\text{true}) = \infty$. The salient feature of Fig. 5 is that progressively more positive R_{us} values yield not only increasing $\cot\phi-\omega^{1/2}$ slopes, but also produce increasingly sub-unity y-intercepts and a noticeable upward curvature in the plots. These features can, at least in principle, be used to distinguish between nonzero $\cot\phi-\omega^{1/2}$ slopes arising from nonzero R_{us} values and from finite electrode kinetics since the plots should always be linear with a y-intercept of unity if the latter, desired, feature dominates.

Solution Resistance Effects at a DME

As noted above, at a non-stationary electrode (most commonly a DME) where the time derivative of the amplitude of the AC current is non-zero, the measurement error can be greater than it would be at a stationary electrode under similar conditions due to the necessary low-pass filter present on the output of the lock-in amplifier.⁷

Figures 2 and 3 also contain a series of plots of $\log k_{ob}^s(\text{app,lim})$ versus $\log R_{us}$ for progressively increasing levels of low-pass filtering. These were computed for a specific solution resistance, ρ , of 10 Ω cm, which corresponds here to $R_s = 17\Omega$. (This ρ value is characteristic of concentrated aqueous electrolytes.) Besides curve A in these figures, which as noted above refers to no filtering, curves B, C, and D refer to 0.03 s, 0.1 s time constant, and two 0.1 s time constants in series, respectively. They show that the additional error in the measurement induced by low-pass filtering is essentially negligible for $R_{us} \geq 2 \Omega$. As $k_{ob}^s(\text{true})$ is decreased to measurable values this error becomes even

smaller. Generally speaking, then, we can conclude that the additional error due to reasonable levels of low-pass filtering can normally be safely neglected in such highly conducting electrolytes.

For less conducting solvents such as most nonaqueous media, however, the situation is quite different. Figure 6 consists of plots of $\log k_{ob}^s(\text{app})$ versus $\log R_{us}$ computed for a markedly higher specific resistance, $\rho = 500 \Omega \text{ cm}$; other chosen parameters are $k_{ob}^s(\text{true}) = 1 \text{ cm s}^{-1}$ and $C_{dl} = 20 \mu\text{F cm}^{-2}$. For $R_{us} \leq 2.5 \Omega$, the error in $k_{ob}^s(\text{app})$ is less than 25% in the absence of low-pass filtering. However, in the presence of as little distortion as provided by a single filter with a 30 ms time constant, if $R_{us} = 0$ this error becomes nearly 40%, and when $R_{us} = 2.5 \Omega$ the value of $k_{ob}^s(\text{app})$ becomes only one half of $k_{ob}^s(\text{true})$. Since the extent of the error caused by the lock-in damping is approximately proportional to the magnitude of the currents involved, these errors will decrease for smaller values of $k_{ob}^s(\text{true})$. For example, with an R_{us} of 1Ω , a $k_{ob}^s(\text{true})$ of 0.5 cm s^{-1} and a 30 ms filter, the error in $k_{ob}^s(\text{app})$ would be only 30%. These effects of lock-in amplifier damping are also seen in the $\log k_{ob}^s(\text{app}) - \log k_{ob}^s(\text{true})$ plots given in Fig. 4; curves B to D refer to the presence of increasing damping, for the same conditions as in Fig. 6.

Decreasing the double-layer capacitance to $5 \mu\text{F cm}^{-2}$, while maintaining the specific resistance at $500 \Omega \text{ cm}$, produces significant changes in the effects of both lock-in damping and uncompensated solution resistance. In the absence of low-pass filtering, for $k_{ob}^s(\text{true}) = 1 \text{ cm s}^{-1}$, up to 5Ω of R_{us} may be present before the error in $k_{ob}^s(\text{app})$ reaches 25%. With a DME, on the other hand, for a 30 ms time constant filter is used only 1Ω of R_{us} needs to be present before a 25% error in

k_{ob}^s (app) is encountered. Again, as k_{ob}^s (true) decreases the situation becomes progressively improved, so that for k_{ob}^s (true) = 0.5 cm s^{-1} , 5Ω or less of uncompensated solution resistance results in less than a 25% error in k_{ob}^s (app), even when a 30 ms filter is employed.

Difficulties in Measuring the Uncompensated Solution Resistance.

The foregoing simulations demonstrate that it is desirable to minimize, or at least have an accurate knowledge of, R_{us} in order to evaluate rapid rate constants with the conventional analysis using AC impedance measurements. In principle, the simplest method of estimating R_{us} is from the cell impedance either at potentials distant from the AC polarographic wave, or in the absence of the electroactive species but using identical iR compensation. In practice, however, the measurement of R_{us} to the desired accuracy (ca. $1\text{--}2 \Omega$) is difficult if not impossible in this fashion. For example, if $C_{dl} = 20 \mu\text{F cm}^{-2}$ we require there to be 3Ω of uncompensated resistance before I_I becomes 1% as large as I_Q even at 1000 Hz. Operating at lower frequencies or with smaller C_{dl} values decreases this fraction even further. Extremely precise I_I measurements are clearly needed even to approximately measure R_{us} . Thus under these conditions, about a 2% change in I_I (equivalent to one degree of phase shift) corresponds to about 5Ω . Such measurements are further complicated by the presence of significant phase distortion in most potentiostats; this places an effective upper limit on the frequencies that can be employed. (We have examined a PAR 174/50, a PAR 173/179, a PAR 273, and a Hi-Tek DT2101 potentiostat and found them all to suffer somewhat in this regard.)

We have described one approach which at least partly circumvents this difficulty.⁶ This involves employing an electronic dummy cell with

components (C_{dl} , R_s) that approximately match those of the actual cell being employed. After achieving the optimal level of iR compensation, the C_{dl} value is increased sufficiently (5 to 20 fold) so that readily measurable I_I values could be obtained, thereby yielding R_{us} from the usual formula $R_{us} = E_{AC}[I_I/(I_Q^2 + I_I^2)]$. (The necessary assumption is, of course, that R_{us} is independent of C_{dl} .)

A number of authors have evaluated rate constants for fast electrode reactions with AC impedance in the presence of large, $\geq 100 \Omega$, values of the uncompensated resistance by measuring the value of R_{us} and subtracting it from the cell response by using the vectorial scheme first described by Randles.⁵ This approach, however, apparently provides no benefits over the use of maximal iR compensation as considered here. Thus even though the measurement of large values of R_{us} can be made with a greater relative precision ($\Delta R/R$) than for small values, the absolute precision is no better. It is clearly the latter which is important in calculating the error in $k_{ob}^s(\text{app})$ arising from the solution resistance.

Experimental Verification

As in practice it is nearly impossible to escape the presence of at least a small amount of uncompensated solution resistance, the effects of lock-in damping upon measured rate constants cannot be examined experimentally in the absence of the influence of R_{us} . Also, as the most reliable rate measurements are made using a DME where problems of surface contamination are minimized, we chose to examine both effects together.

Our approach was to select a redox couple, cobalticinium-cobaltocene ($\text{Cp}_2\text{Co}^{+/0}$), that exhibits relatively well-defined, yet measurable, electrode kinetics at the DME in a number of nonaqueous solvents.¹² By

using low mercury flow rates, long drop times, minimal lock-in filtering, and maximal iR compensation the corrections that are necessary to apply to $k_{ob}^s(app)$ so to yield $k_{ob}^s(true)$ can be arranged to be moderate or minor. For example, in dimethylsulfoxide (DMSO) containing 0.1 M tetrabutylammonium hexafluorophosphate we obtain $k_{ob}^s(true) = 0.7 \text{ cm s}^{-1}$, the corresponding $k_{ob}^s(app)$ values being only 20-30% smaller.

Using a DME of higher flow rate, 2.6 mg s^{-1} , and a larger amplifier time constant, 0.1 s, we then determined $k_{ob}^s(app)$ as a function of R_{us} . To do this, we obtained values of $k_{ob}^s(app)$ for $\text{Cp}_2\text{Co}^{+/0}$ at maximal iR compensation (i.e. minimal R_{us} , at the setting just prior to potentiostat oscillation) and then diminished the compensation level to be 10, 20, and then 50 Ω below this point. (See ref. 12 for experimental details.) A comparison between the resulting $k_{ob}^s(app)$ values and those simulated from the additional R_{us} values using the above procedure is given as a function of R_{us} in Fig. 7: the points denote the experimental values and the curve is obtained from the digital simulations. The observed reasonable agreement between the experimental points and the simulated curve supports the underlying validity of the present analysis.

Consequently, each of the measured $k_{ob}^s(app)$ values in Fig. 7 can be used to estimate $k_{ob}^s(true)$ for this system with reasonable accuracy, by evaluating R_{us} and using the known experimental parameters (C_{dl} , ρ , etc.) to simulate a series of corresponding values of $k_{ob}^s(app)$ and $k_{ob}^s(true)$, as exemplified in Fig. 4. The correct value of $k_{ob}^s(true)$ will be that corresponding to the $k_{ob}^s(app)$ value that best matches the experimental quantity. Besides providing a quantitatively reliable estimate of $k_{ob}^s(true)$, this procedure has the critical virtue of yielding

an assessment of the maximum rate constant that can be evaluated with a given instrument and experimental technique.

An alternative scheme for accounting for the effects of solution resistance and amplifier damping would be to correct the measured AC currents themselves. However, since these combined effects influence the currents in a complex manner, the approach followed here has the advantage of greater simplicity.

Concluding Remarks

Both the uncompensated solution resistance and, at a DME, the amplifier low-pass filter act to distort AC impedance data in such a way to make the apparent observed rate constant uniformly smaller than the actual value. The effects of these two factors are interactive rather than simply additive, and always combine together to yield an error in $k_{ob}^s(\text{app})$ that is larger than that resulting from either of the individual factors alone. Since the magnitude of the distorting effects of the amplifier damping depend upon the total solution resistance rather than the uncompensated portion alone, these effects will be retained even if $R_{us} = 0$.

This situation might be regarded as presenting a bleak picture for the evaluation of fast electrode kinetics, at least using conventional AC impedance measurements. However, the same simulations that are used to diagnose the presence of such deleterious effects can also be utilized to improve the accuracy by which moderately fast rate constants can be evaluated.

Acknowledgment

This work is supported by the Office of Naval Research.

References

1. J. E. B. Randles and K. W. Somerton, *Trans. Far. Soc.* 48 (1952), 937, 951.
2. D. F. Calef and P. G. Wolynes, *J. Phys. Chem.* 87 (1983), 3387.
3. (a) D. E. Smith, in *Electroanalytical Chemistry*, Vol. 1, A. J. Bard, ed., M. Dekker, New York, 1970, p. 1; (b) D. E. Smith, *Crit. Rev. Anal. Chem.* 2 (1971), 247.
4. M. Sluyters-Rehbach and J. H. Sluyters, *Comprehensive Treatise of Electrochemistry*, Vol. 9, E. Yeager, J. O'M. Bokris, B. E. Conway, and S. Sarangapani, eds., Plenum, New York, 1984, Chapter 4.
5. J. E. B. Randles, *Disc. Far. Soc.* 1 (1947), 11.
6. D. Milner and M. J. Weaver, *J. Electroanal. Chem.* 191 (1985), 41.
7. D. F. Milner and M. J. Weaver, *Anal. Chim. Acta*, submitted.
8. For example, R. de Levie and L. Pospisil, *J. Electroanal. Chem.* 22 (1969), 277.
9. P. E. Whitson, H. W. Vander Born, and D. H. Evans, *Anal. Chem.* 45 (1973), 1298.
10. P. Horowitz and W. Hill, "The Art of Electronics", Cambridge University Press, Cambridge, 1980, Chapter 1.
11. E. R. Brown, D. E. Smith, and G. L. Booman, *Anal. Chem.* 40 (1968), 1411.
12. (a) T. Gennett, D. F. Milner, and M. J. Weaver, *J. Phys. Chem.* 89 (1985), 2787. (b) G. E. McManis, N. Golovin, and M. J. Weaver, *J. Phys. Chem.*, in press.

Figure Captions

Fig. 1

Equivalent circuit of electrochemical cell employed for simulations.

Fig. 2

Logarithm of limiting value of $k_{ob}^s(\text{app})$ [i.e. value of $k_{ob}^s(\text{app})$ when $k_{ob}^s(\text{true}) = \infty$], $\log k_{ob}^s(\text{app}, \text{lim})$ plotted against logarithm of uncompensated resistance, $\log R_{us}$. Simulation conditions are $C_{dl} = 5 \mu\text{F cm}^{-2}$ and $\rho = 10 \Omega \text{ cm}$. Curve A refers to no low-pass filtering; curves B-D for filter time constants equal to 0.03 s, 0.1 s, and for a pair of 0.1 s filters in series.

Fig. 3

As for Fig. 2, but for $C_{dl} = 20 \mu\text{F cm}^{-2}$.

Fig. 4

Plots of logarithm of apparent (measured) rate constant, $\log k_{ob}^s(\text{app})$, against logarithm of corresponding "true" value, $\log k_{ob}^s(\text{true})$, for $C_{dl} = 20 \mu\text{F cm}^{-2}$ and $\rho = 500 \Omega \text{ cm}$. Damping conditions for curves A-D as in Fig. 2.

Fig. 5

The cotangent of the phase angle attributed to faradaic current, $\cot\phi$, (see text) plotted against square root of AC frequency, $\omega^{1/2}$, for various R_{us} values, with $C_{dl} = 20 \mu\text{F cm}^{-2}$. Straight lines shown are least squares best fits to points. Key to R_{us} values: \square , 0 Ω ; ∇ , 0.5 Ω ; \diamond , 1 Ω ; Δ , 2 Ω .

Fig. 6

Plots of $\log k_{ob}^s(\text{app})$ versus $\log R_{us}$ for $k_{ob}^s(\text{true}) = 1 \text{ cm s}^{-1}$, $C_{dl} = 20 \mu\text{F cm}^{-2}$; $\rho = 500 \Omega \text{ cm}$. Damping conditions for curves A-D as in Fig. 2.

Fig. 7

Experimental values of $k_{ob}^s(\text{app})$ for $\text{Cp}_2\text{Co}^{+/0}$ in dimethylsulfoxide (containing 0.1 M tetrabutylammonium hexafluorophosphate) obtained at a DME (solid points) as a function of the uncompensated solution resistance, using a lock-in amplifier time constant of 0.1 s. Solid curve is corresponding simulated data obtained for $k_{ob}^s(\text{true}) = 0.7 \text{ cm s}^{-1}$. (See text for further details.)

END

DATE

FILMED

6-1988

DTIC